Millimeter-Wave Short-Focus Thin Lens Employing Disparate Filter Arrays

Jungsuek Oh, *Member, IEEE*

***Abstract*—This letter presents a millimeter-wave thin lens employing disparate filter arrays created by placing both metallic patches and wire mesh on the same plane. This disparate configuration of patches and wire mesh enables the coexistence of two different types of filter response, lowpass and bandpass, on the same plane. It is found that this disparate design can achieve improvement in the tunable range of phase shift of the spatial filter array with a limited number of metal and substrate layers so as to retain the thin feature of the lens. This arrangement enables higher focusing gain than prior thin lenses employing single-type spatial filter arrays for a short focus of $f/\mathrm{D} = 0.2$, where f is the focal length and D is the lateral dimension (aperture) of the lens. The design procedure for the proposed lens employing the disparate filter arrays is discussed. Full-wave simulation results demonstrate that the proposed lens can achieve more than 2 dB in gain enhancement over previous thin lenses made of only lowpass filter arrays. The fabricated lens is confirmed to have less than $0.05\ \lambda_0$ in total thickness and up to 11 dB in gain for $f/\mathrm{D} = 0.2$.**

***Index Terms*—Bandpass filter, lens, lowpass filter, millimeter-wave antennas.**

I. Introduction

LENSES have been widely used in many applications operating from microwave to optical frequencies. A significant amount of research regarding dielectric lenses has been conducted to allow for beam steering and shaping applications at these lower frequencies [1]–[4]. Recent advancements in frequency selective surfaces (FSSs) and metasurface technology have enabled the emergence of thin flat lenses for microwave frequencies [5]–[10]. For such lenses with electrically large apertures, selection of millimeter-wave frequencies (between microwave and optical frequencies) is a feasible compromise for industrial products because the advantage of the electrically-large-aperture effect is still valid at millimeter-wave frequencies, although the lenses do not require the physically bulky features of microwave lenses.

To apply this thin lens technology to millimeter-wave applications, there are many technical barriers in terms of system integration, fabrication, and functionality [11]. The lenses need to have the ability to be integrated into millimeter-wave system packages. This integration configuration limits not only the lens thickness, but also the distance between the antenna and the lens, so as to produce a small system volume. Because the distance between the antenna and the lens is determined by the inherent focal length of the lens, integration capability requires a short focal length along with thinness. f/D is used extensively as an effective criterion of the focal length, where f is the focal length and D is the lateral dimension of the lens.

The letter presents a novel design technique that can improve the gain of millimeter-wave short-focus thin lenses by placing two different filter responses on the same lens surface. In the lens, one type of unit cell consists of only patches, while another type consists of both patches and wire mesh. In the second metal layer, the patches and wire mesh coexist to produce a wider tunable range of phase shift; this results in gain enhancement for short-focus thin lenses. In Section II, disparate phase features of two different-type unit cells, corresponding to lowpass and bandpass response, are demonstrated. In Section III, based on the unit cell analysis, a design procedure for a flat thin lens is discussed. In Section IV, full-wave simulation and measurement results confirm the advantages of the proposed design approach for short-focus thin lenses.

II. Disparate filter arrays

Discussion of the proposed design approach starts from two well-known FSS unit cells functioning as spatial lowpass and bandpass filters, respectively. The geometrical shapes and design parameters of the two unit cells are shown in Fig. 1. The geometrical difference between lowpass and bandpass unit cells is that lowpass unit cells consist of only patches and bandpass unit cells consist of both patches and wire mesh. To perceive the wire-mesh pattern clearly, note that the repetition of the loop-shape unit pattern in Fig. 1(b) produces the wire-mesh pattern highlighted in Fig. 6(b) [12]. In the past, the design of thin lenses has relied on a single-type unit cell, namely a lowpass or bandpass unit cell. In the literature, the necessary wide range of phase shift is acquired by increasing the order of the filter response. However, this requires a significant increase in the number of metal and substrate layers. This stacked-layer configuration may be acceptable for microwave lenses, but not for millimeter-wave lenses because of the increased energy loss and fabrication errors resulting from misalignment among the metal layers between bonding layers and because of the increased fabrication cost. To address this, a new design method combining different-order lowpass elliptic filter responses was reported [11]. The literature demonstrates promising results when f/D is 0.7. However, only relying on the same type of

Manuscript received July 17, 2015; accepted December 14, 2015. Date of publication December 28, 2015; date of current version May 12, 2016. This work was supported by Inha University under Research Grant INHA-51369 and Samsung Electronics.

The author is with the Department of Electronic Engineering, Inha University, Incheon 402-751, South Korea (e-mail: jungsuek@inha.ac.kr).

Color versions of one or more of the figures in this letter are available online at http://ieeexplore.ieee.org.

Digital Object Identifier 10.1109/LAWP.2015.2512853

1536-1225 © 2015 IEEE. Personal use is permitted, but republication/redistribution requires IEEE permission.
See http://www.ieee.org/publications_standards/publications/rights/index.html for more information.

Authorized licensed use limited to: Seoul National University. Downloaded on December 15,2022 at 13:34:48 UTC from IEEE Xplore. Restrictions apply.

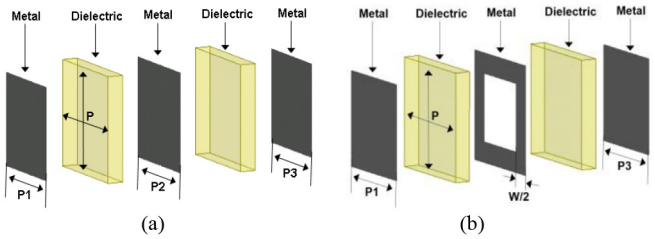

Fig. 1. Exploded view and dimension parameters of (a) lowpass and (b) bandpass unit cells.

TABLE I
DIMENSION PARAMETERS, PHASE SHIFT, AND INSERTION LOSS OF LOWPASS AND BANDPASS UNIT CELLS AT 28 GHZ WITH NORMAL INCIDENCE

UC#	Filter Type	P1 and P3 (mm)	P2 (mm)	W (mm)	Phase (degree)	Insertion Loss (dB)
1	Lowpass	1.275			-117	1.5
2	Lowpass	1.3			-130	1.2
3	Lowpass	1.325			-145	0.4
4	Lowpass	1.325	1.5		-169	1.9
5	Lowpass	1.35	1.5		-192	0.81
6	Lowpass	1.375	1.5		-211	0.4
7	Lowpass	1.4	1.5		-247	0.9
8	Lowpass	1.425	1.5		-262	1.5
9	Lowpass	1.45	1.5		-278	1.4
10	Bandpass	0.85		0.6	17	2
11	Bandpass	0.9		0.6	2	1
12	Bandpass	0.95		0.6	-20	0.4
13	Bandpass	1		0.6	-40	0.5
14	Bandpass	1.05		0.6	-58	1.3
15	Bandpass	1.1		0.6	-74	1.9
16	Bandpass	1.15		0.6	-85	2
17	Bandpass	1.2		0.6	-95	2.1

filter response limits lens gain for short focusing when f/D is 0.2, which is addressed in this letter. The numbers of metal and substrate layers are limited to three and two, respectively, for a practical implementation at millimeter-wave frequencies. Rogers 6010LM and 2929 Bondply are used as the substrate and bonding layers, respectively. Permittivity, loss tangent, and thickness (mm) of Rogers 6010LM and 2929 Bondply are 10.2, 0.0023, and 0.254 and 2.94, 0.003, and 0.04, respectively. Because a lowpass filter array (LFA) requires a smaller number of metal and substrate layers than a bandpass filter array (BFA) for the same tunable range of phase shift, the LFA is considered as a reference for the proposed disparate filter arrays (DFAs). Three stacked patch layers in Fig. 1(a) can create 3rd- and 5th-order lowpass filter responses [11]. The unit cells are designed to have less than 3 dB of insertion loss (IL) at 28 GHz and to achieve a maximum available tunable range of phase shift within the 3-dB IL bandwidth.

In this letter, unit cells with the dimension of 1.6×1.6 mm^2 contain different-sized patches; they are numbered as listed in Table I. The phase shift and transmittance are shown Figs. 2–4. Note that the tunable range of phase shift of the LFA cannot cover from -120° to $+80^\circ$, as indicated by the shadowed area in Fig. 2. As will be discussed in Section IV, this uncovered region may cause quantization loss in the lens, leading to a decrease in lens (focusing) gain that is pure gain enhancement

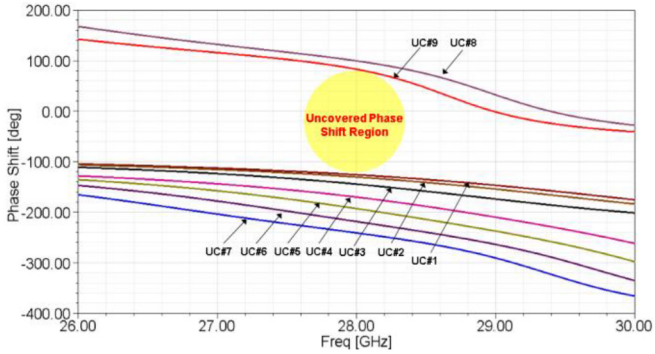

Fig. 2. Simulated phase shift through lowpass unit cells with different patch sizes. (The shadowed area indicates the uncovered region of phase shift, which is unable to fully collimate propagating rays through the thin lens.)

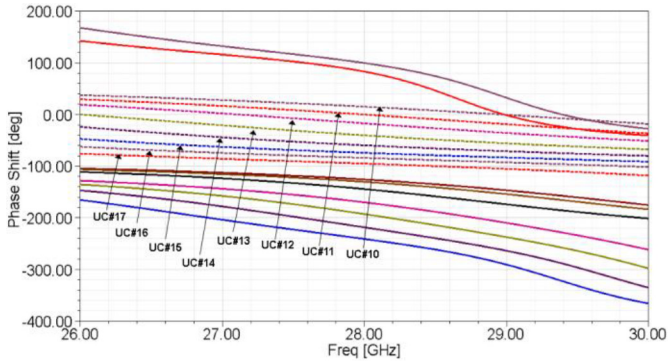

Fig. 3. Simulated phase shift of both lowpass and bandpass unit cells with different patch sizes and wire mesh widths.

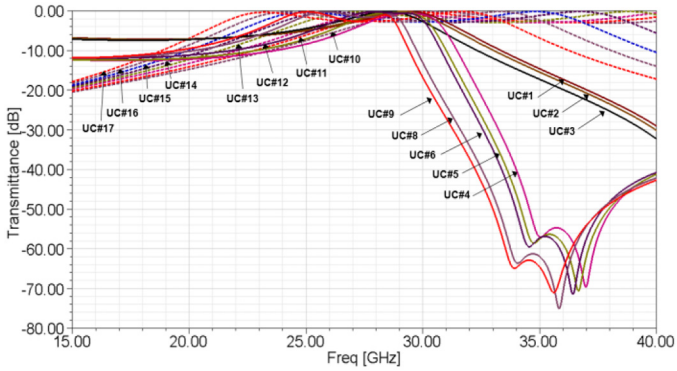

Fig. 4. Simulated transmittance (S_{21}) of both lowpass and bandpass unit cells with different-sized patches and different-width wire mesh.

factor [dB] by the lens. Fig. 3 depicts a key idea of this letter by adding the tunable range of the phase shift of the BFA shown in Fig. 1(b) to Fig. 2. This DFA, made of an LFA and a BFA, can broaden the tunable range of the phase shift within 3 dB IL bandwidth by covering the shadowed region in Fig. 2. Fig. 4 confirms that all of the LFA and BFA unit cells have insertion loss of less than 3 dB at 28 GHz.

III. LENS DESIGN

In this section, utilizing the tunable range of phase shift enhanced by the proposed disparate filter arrays, a flat thin

Authorized licensed use limited to: Seoul National University. Downloaded on December 15,2022 at 13:34:48 UTC from IEEE Xplore. Restrictions apply.

TABLE II
NUMBERED ZONES, REQUIRED PHASE SHIFT AT THE CENTER OF EACH ZONE, SELECTED UC# FOR EACH ZONE, INCIDENT ANGLE, PHASE, AND INSERTION LOSS AT THE CENTER OF EACH ZONE

Zone	Required phase shift at the center of each zone (degree)	Selected UC#	Incident angle at the center of each zone (degree)	Phase of unit cell with normal incidence (degree)	Phase of unit cell at the center of each zone (degree)	Insertion Loss of unit cell with normal incidence (dB)	Insertion Loss of unit cell at the center of each zone (dB)
z1	-130	2	0	-130	-130	1.2	1.2
z2	-111	1	17	-117	-120	1.5	1.8
z3	-30	12	32	-20	-13	0.4	0.4
z4	-295	9	43	-278	-275	1.4	1.9
z5	-207	6	52	-211	-209	0.4	0.5
z6	-101	17	57	-95	-91	2.1	2.8
z7	0	11	62	2	19	1	1.8
z8	-247	7	65	-247	-243	0.9	2.1
z9	-151	3	68	-145	-118	0.4	2.7

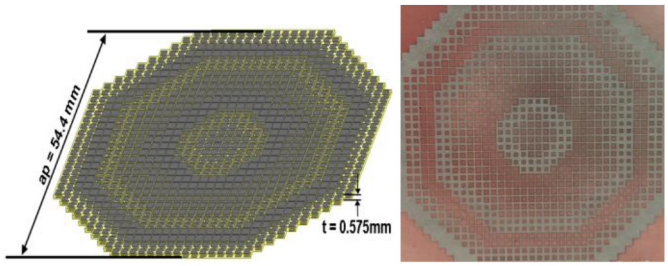

Fig. 5. (a) Simulation model and (b) fabricated sample of the proposed lens.

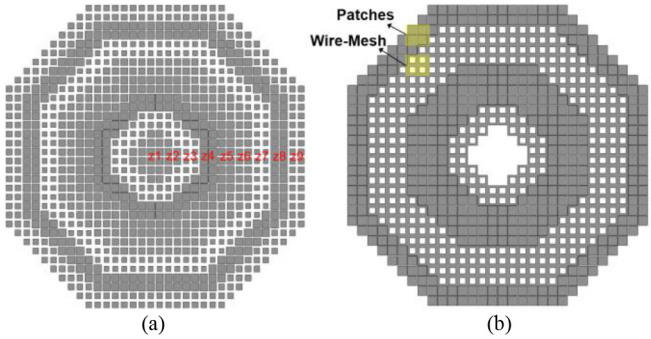

Fig. 6. Top view of (a) first and third metal layers and (b) second metal layers configured using coplanar patches and wire mesh.

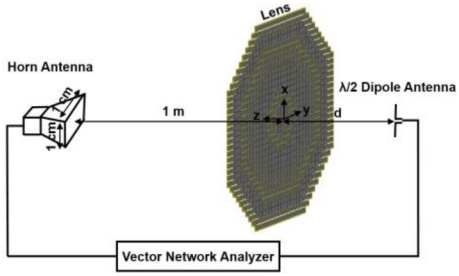

Fig. 7. Measurement setup to characterize the focusing features of the lens.

lens is designed. The lens design follows the generic procedure described in the literature [8], [11]. First, the phases of spherical waves emitted by a $\lambda/2$ dipole antenna are captured on the aperture of 54.4×54.5 mm^2 at the distance of 10 mm from the antenna. The 10-mm distance is selected to realize the short-focus designs that allow f/D to be 0.2. From the captured phase values, the amount of phase shift with a surface resolution of 1.6 mm ($=$ unit cell size) that is required to transform the emitted spherical waves into plane waves is calculated. The unit cell number (UC#) with the phase shift value that is closest to the calculated values is selected from Table I. In this way, the lens aperture is filled with a disparate filter array made up of the selected unit cells.

Table II shows the numbered zones, required phase shift at the center of each zone, selected UC# for each zone, incident angle, phase, and insertion loss at the center of each zone. From comparison between the fifth and sixth columns in Table II, it is assumed that variations in phase and insertion loss by different incident angle are small. Finally, a lens structure is designed as shown in Fig. 5(a). The lateral dimension of the lens ($=$ ap) is 54.5 mm, and total thickness of the lens is 0.575 mm based on the sum of thickness of two Rogers 6010 ($= 0.254$ mm $\times$ 2) layers, one 2929 Bondply ($= 0.04$ mm) layer, and three copper claddings ($= 0.009$ mm $\times$ 3).

Fig. 5(b) shows a photograph of fabricated sample of the proposed lens. As stated above, the proposed lens consists of three metal layers, two substrates (Rogers 6010), and one bonding layer (2929 Bondply). Fabrication process starts from printing metallic patterns on the top and bottom copper claddings of the first substrate corresponding to the first and second metal layers. Next, metallic patterns for the third metal layer are printed on the bottom copper cladding of the second substrate. Finally, the bottom side of the first substrate (where second metal layer exists) is combined with the top side of the second substrate (where no metallic pattern exists) through a bonding layer with pressure and heat. The metallic patterns on the first and third metal layers are the same as those shown in Fig. 6(a). Unlike those of the first and third metal layers, the metallic patterns on the second metal layer have both patches and wire mesh, which correspond to lowpass and bandpass filter arrays, respectively, forming the DFA. Fig. 6(b) shows the coplanar patches and wire mesh.

IV. SIMULATION AND MEASUREMENT RESULTS

The structure of the proposed thin lens was full-wave simulated with ANSYS HFSS for performance characterization. Fig. 7 shows the setup used for both simulation and measurement activities. In the setup, a $\lambda/2$ dipole antenna and a horn antenna are connected to a vector network analyzer; the proposed lens is positioned in front of the dipole antenna, and the distance between the lens and the horn antenna is 1 m. The lens is mounted in a jig, which can adjust the distance between the lens and the dipole antenna. Energy is transmitted from the dipole antenna for two cases: with and without the lens. From the difference between the received powers at the horn antenna for the cases of with and without the lens, the gain of the lens is extracted. To measure the focal length of the lens ($= f/\mathrm{D}$), the distance between the lens and the antenna at which the max lens gain is acquired should be determined. Therefore, the

Authorized licensed use limited to: Seoul National University. Downloaded on December 15,2022 at 13:34:48 UTC from IEEE Xplore. Restrictions apply.

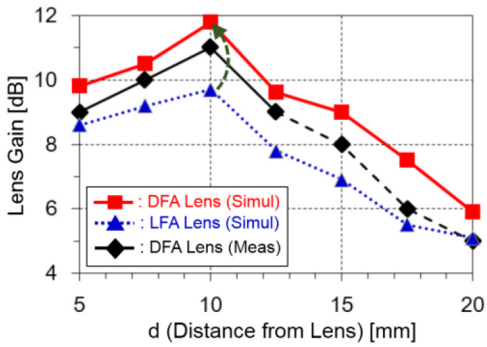

Fig. 8. Simulated and measured lens gains for DFA and LFA lenses.

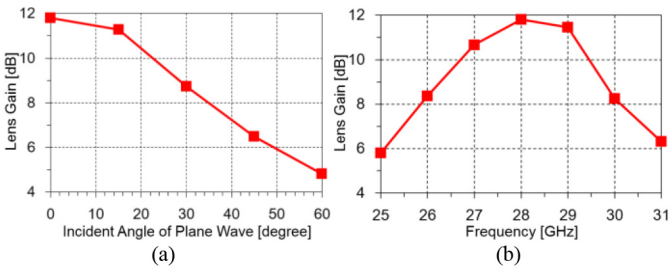

Fig. 9. Simulated lens gain of DFA lens as a function of (a) incident angle of plane wave and (b) frequency.

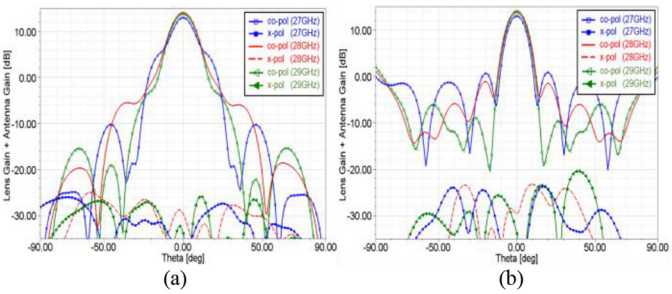

Fig. 10. Radiation patterns of DFA lens fed by $\lambda/2$ dipole antenna in the (a) xz-plane and (b) yz-plane (x-, y-, and z-axis are shown in Fig. 7).

aforementioned measurement is performed multiple times for different distances between the lens and the dipole antenna near the expected focal length.

Fig. 8 shows the simulated and measured lens gains for the proposed DFA-based lens and simulated lens gain of the prior LFA-based lens as a function of the distance between the lens and the dipole antenna. The LFA lens is used as a reference; the lens consists of only LFA, while the presented DFA does both LFA and BFA. The type and number of substrate and bonding layer, total thickness, and aperture size in the LFA lens are the same as those of the presented DFA lens for fair comparison. For all three datasets in Fig. 8, the focal length is observed to be 10 mm. By comparing the simulated results of DFA and LFA lenses, it is demonstrated that the increased tunable range of phase shift of the DFA can result in gain enhancement (≈ 2 dB) for a case of short focus ($f/\mathrm{D} \approx 0.2$). Fig. 9(a) shows simulated lens gains by different incident angle of plane wave. Overall results are within about 2 dB difference from the results in [8]. Fig. 9(b) shows simulated lens gain as a function of frequency. This suggests 3-dB gain bandwidth is about 13%, which is lower than the bandwidth ($= 20\%$) reported in [8]. This is due to thinner configuration ($= 0.05\lambda_0$) of the proposed lens, compared to the thickness ($= 0.08\lambda_0$) of the previous thin lens reported in [8]. Fig. 10 shows radiation patterns of DFA lens fed by $\lambda/2$ dipole antenna at 27, 28, and 29 GHz in the xz- and yz-planes.

V. Conclusion

A novel design approach to achieve high focal gain for millimeter-wave short-focus thin lenses is presented. It is demonstrated that disparate filter array configured by using subwavelength unit cells can achieve gain enhancement for short-focus thin lenses at 28 GHz. All of the unit cells constituting the filter arrays are designed considering feasible printed circuit board (PCB) processes at millimeter-wave frequencies. Finally, the simulated and measured results demonstrate the expected performance and features of the proposed lens.

References

[1] J. R. Costa, E. B. Lima, and C. A. Fernanders, "Compact beam-steerable lens antenna for 60 GHz wireless communications," *IEEE Trans. Antennas Propag.*, vol. 57, no. 10, pp. 2926–2933, Oct. 2009.

[2] J. Thomton, "Properties of spherical lens antennas for high altitude platform communications," *Proc. 6th Eur. Workshop Mobile/Pers. Satcoms & 2nd Adv. Satell. Mobile Syst. Conf.*, Sep. 21–22, 2004.

[3] B. Chantraine-Bares, R. Sauleau, L. Le Coq, and K. Mahdjoubi, "A new accurate design method for millimeter-wave homogeneous dielectric substrate lens antennas of arbitrary shape," *IEEE Trans. Antennas Propag.*, vol. 53, no. 3, pp. 1069–1082, Mar. 2005.

[4] M. G. M. V. Silveirinha, and C. A. Fernandes, "Shaped double-shell dielectric lenses for wireless millimeter wave communications," *IEEE AP-S Int. Symp. Dig.*, 2000, vol. 3, pp. 1674–1677.

[5] A. Abbaspour-Tamijani, K. Sarabandi, and G. M. Rebeiz, "Antenna-filter-antenna arraysas a class of bandpass frequency-selective surfaces," *IEEE Trans. Microw. Theory Tech.*, vol. 52, no. 8, pp. 1781–1789, Aug. 2004.

[6] A. Abbaspour-Tamijani, K. Sarabandi, and G. M. Rebeiz, "A millimetre-wave bandpass filter lens array," *Microw., Antennas Propag.*, vol. 1, no. 2, p. 388, Apr. 2007.

[7] N. Behdad and M. Al-Joumayly, "A generalized synthesis procedure for low-profile frequency selective surfaces with odd-order bandpass responses," *IEEE Trans. Antennas Propag.*, vol. 58, no. 7, pp. 2460–2464, Jul. 2010.

[8] M. A. Al-Joumayly and N. Behdad, "Wideband planar microwave lenses using sub-wavelength spatial phase shifters," *IEEE Trans. Antennas Propag.*, vol. 59, no. 12, pp. 4542–4552, Dec. 2011.

[9] C. Pfeiffer and A. Grbic, "Millimeter-wave transmitarrays for wavefront and polarization control," *IEEE Trans. Microw. Theory Tech.*, vol. 61, no. 12, pp. 4407–4417, Dec. 2013.

[10] N. Gagnon, A. Petosa, and D. A. McNamara, "Printed hybrid lens antenna," *IEEE Trans. Antennas Propag.*, vol. 60, no. 5, pp. 2514–2518, May 2012.

[11] J. Oh, "Millimeter wave thin lens employing mixed-order elliptic filter arrays," *IEEE Trans. Antennas Propag.*, 2016, to be published.

[12] J. Oh and K. Sarabandi, "A topology-based miniaturization of circularly polarized patch antennas," *IEEE Trans. Antennas Propag.*, vol. 61, no. 3, pp. 1422–1426, Mar. 2013.

Authorized licensed use limited to: Seoul National University. Downloaded on December 15,2022 at 13:34:48 UTC from IEEE Xplore. Restrictions apply.